Catalysis Today 181 (2012) 116–123

Contents lists available at ScienceDirect

Catalysis Today

journal homepage: www.elsevier.com/locate/cattod

NO_2 uptake under practically relevant conditions on BaO/Pt(1 1 1)

Kumudu Mudiyanselage, János Szanyi*

Institute for Interfacial Catalysis, Pacific Northwest National Laboratory, P.O. Box 999, MSIN: K8-87, Richland, WA 99352, USA

ARTICLE INFO

Article history:
Received 18 February 2011
Received in revised form 25 April 2011
Accepted 27 May 2011
Available online 25 June 2011

Keywords:
Model NSR catalysts
NO_2 uptake
Disordered/ordered nitrate phase

ABSTRACT

The formation of nitrites and nitrates ($Ba(NO_x)_2$) under practically relevant conditions (P_{NO_2} up to 1.0 Torr and T = 500 K) and their thermal decomposition on BaO (>20 monolayer equivalent (MLE))/Pt(1 1 1) were studied using temperature programmed desorption (TPD), infrared reflection absorption (IRA), and X-ray photoelectron (XP) spectroscopies. The exposure of BaO to 1.0×10^{-8} Torr NO_2 at 500 K leads to the formation of a $Ba(NO_x)_2$ layer with small, disordered crystalline nitrate clusters. Under these conditions ($P_{NO_2} = 1.0 \times 10^{-8}$ Torr and T = 500 K) only the top portion of the BaO layer converts to $Ba(NO_x)_2$ and the nitrites in this $Ba(NO_x)_2$ layer stay without converting completely to nitrates even after 100 min of NO_2 exposure. In the thermal decomposition of $Ba(NO_x)_2$, first nitrites decompose, releasing NO and then the decomposition of nitrates occurs via two pathways releasing NO_2 and $NO + O_2$. At 500 K and $P_{NO_2} \geq 1.0 \times 10^{-7}$ Torr, first NO_2 reacts with BaO to form small disordered crystalline $Ba(NO_3)_2$ particles and then these particles agglomerate to form large, well-ordered (bulk-like) crystalline nitrates as the NO_2 exposure increases. The thermal decomposition of these well-ordered, bulk-like crystalline nitrate aggregates occurs in two steps releasing NO_2 and $NO + O_2$ in each step in two different temperature regions. NO_2 pressure $\geq 1.0 \times 10^{-5}$ Torr is required for the complete oxidation of initially formed nitrites to nitrates and the full nitration of the BaO layer at 500 K sample temperature.

Published by Elsevier B.V.

1. Introduction

Understanding the formation and decomposition mechanisms of Ba-nitrites and Ba-nitrates ($Ba(NO_x)_2$) on model systems is essential to develop more efficient NO_x storage and reduction (NSR) automotive catalysts. Many studies have reported on the reactions of NO_2 with BaO, the active storage component in the NSR catalyst, deposited on oxide thin films (e.g., Al_2O_3/NiAl(1 1 0) [1–6]), as well as on metal single crystals (e.g., Pt(1 1 1) [7–11] and Cu(1 1 1) [12]). Some of these studies have suggested that the substrate of model systems played a significant role in the formation and decomposition processes of $Ba(NO_x)_2$ due, mainly, to the strong interactions between the substrate and BaO/$Ba(NO_3)_2$ [4,13–15]. In order to understand the effects the substrate may play on the formation and decomposition of $Ba(NO_x)_2$, data obtained from the model systems with and without the influence from the underlying substrate should be compared. To obtain such information without the influence from the underlying substrate, experiments should be performed on model systems with relatively thick BaO layers. In addition, these experiments on model systems need to be performed under practically relevant conditions to render the results obtained from the model studies relevance to processes on the NSR catalysts operated under practical conditions. To this end, we performed experiments on a model system with a thick BaO (>20 monolayer equivalent (MLE)) film supported on Pt(1 1 1) to investigate the formation of nitrite and nitrate species at elevated pressures (up to 1.0 Torr) and temperature (500 K). The thick layer in this system ensures that the chemistry of BaO is unaffected by the Pt substrate. Subsequently, we also investigated the decomposition processes of the thus formed $Ba(NO_x)_2$ in temperature programmed desorption (TPD) experiments.

The formation of $Ba(NO_x)_2$ under NO_2 atmosphere has been studied on BaO/Al_2O_3/NiAl(1 0 0) [16], BaO/Al_2O_3/NiAl(1 1 0) [5,6,13], and BaO/Pt(1 1 1) [9,11] model systems at different BaO film thicknesses under ultra-high vacuum (UHV) conditions ($P_{NO_2} \sim 1.0 \times 10^{-9}$ Torr) in a wide temperature range (90–660 K). In addition, the formation of amorphous $Ba(NO_3)_2$ following the exposure of BaO(>30 (MLE))/Al_2O_3/NiAl(1 1 0) [17] and BaO(>20 MLE)/Pt(1 1 1) [11] to elevated NO_2 pressure (~up to 1.0 Torr) at 300 K, and its conversion to a crystalline form upon annealing to 500 K in the absence of NO_2 were also observed in previous studies [11,17]. Although, many studies have investigated the reaction of NO_2 with BaO deposited on oxide thin films [1–6] and metal single crystals [7–12], to the best of our knowledge, the formation of nitrites and nitrates on a relatively thick BaO layer in a single crystal based model system at elevated pressures and temperatures has not been reported previously. Here we present the results of the reaction of NO_2 with BaO(>20 MLE)/Pt(1 1 1) at elevated pressure

* Corresponding author. Tel.: +1 509 371 6524; fax: +1 509 371 6242.
E-mail address: janos.szanyi@pnl.gov (J. Szanyi).

0920-5861/$ – see front matter. Published by Elsevier B.V.
doi:10.1016/j.cattod.2011.05.033

and temperature and show the formation of a well-ordered, bulk crystalline $Ba(NO_3)_2$ layer, and its subsequent two-step decomposition process.

2. Experimental

All the experiments were performed in a combined UHV surface analysis chamber and elevated-pressure reactor/infrared reflection absorption spectroscopy (IRAS) cell system with a base pressure of less than 2.0×10^{-10} Torr [1 Torr = 1.3332 mbar]. The UHV chamber is equipped with X-ray photoelectron spectroscopy (XPS), low energy electron diffraction (LEED), and TPD techniques. The elevated-pressure cell is coupled to a commercial Fourier transform infrared (FT-IR) spectrometer (Bruker, Vertex 70). The Pt(1 1 1) single crystal (10 mm diameter, 2 mm thick, Princeton Scientific) used in these experiments was spot-welded onto a U-shaped Ta wire, and the sample temperature was measured by a C-type thermocouple spot-welded to the backside of the crystal. The Pt(1 1 1) crystal was cleaned by repeated cycles of Ar^+ ion sputtering and annealing in O_2 at 800 K. The cleanliness of the surface was verified with XPS, and LEED. The thick (>20 MLE) BaO film was prepared by reactive layer-assisted deposition (RLAD); first the desired amount of Ba was deposited onto a N_2O_4 multilayer on the clean Pt(1 1 1) crystal at 90 K by physical vapor deposition using a resistively heated Ba doser (SAES Getters), and then the thus formed BaN_xO_y layer was thermally decomposed by annealing to 1000 K. The obtained BaO film was characterized by XPS. (No binding energy (BE) shift was observed as a result of sample charging during the XPS measurements, therefore, all the data reported in the figures are raw data without any correction.) NO_2 was purified by several cycles of freeze/pump/thaw prior to use. IR spectra were collected at 4 cm^{-1} resolution using a grazing angle of approximately 85° to the surface normal. All the IR spectra collected were referenced to a background spectrum acquired from the clean sample prior to gas adsorption. After the completion of IRAS experiments in the elevated-pressure reactor/IRAS cell, the sample was moved to the UHV chamber for XPS and TPD experiments to identify the species on the sample surface and to determine their coverages. The heating rate used in all the TPD experiments was 2 K s^{-1}.

3. Results and discussion

3.1. Formation of $Ba(NO_x)_2$ at $P_{NO_2} = 1.0 \times 10^{-8}$ Torr and T = 500 K

The formation of $Ba(NO_x)_2$ on BaO/Pt(1 1 1) was investigated first at 1.0×10^{-8} Torr NO_2 pressure and 500 K sample temperature, and IR spectra were collected as a function of time (146 spectra in 100 min) during NO_2 exposure. Fig. 1a shows contour plots of the IR spectra collected in the frequency range of 1150–1550 cm^{-1} (contour plots were created from the series of IR spectra recorded using Origin software). The IR peaks observed at 1243 and 1412 cm^{-1} can readily be assigned to nitrites and nitrates, respectively, based on previously reported values [1–3,5,6,15,17,18]. The intensities of the IR peaks for both nitrite and nitrate species gradually increase with increasing NO_2 exposure time. Note that no saturation of the BaO layer was achieved even after 100 min of NO_2 exposure, although the rates of IR signal intensity increases were very low at long exposure times. At $P_{NO_2} = 1.0 \times 10^{-8}$ Torr, only the top portion of the BaO layer converted to $Ba(NO_x)_2$ and the proceeding of the reaction to form more $Ba(NO_x)_2$ slowed down dramatically due, most likely, to the limited diffusion of NO_2 through the top nitrite/nitrate layer to reach the underlying BaO. The N 1s XP spectrum obtained after the 100 min exposure of BaO/Pt(1 1 1) to NO_2 ($P_{NO_2} = 1.0 \times 10^{-8}$ Torr; T = 500 K) shows two peaks at 407.6 and

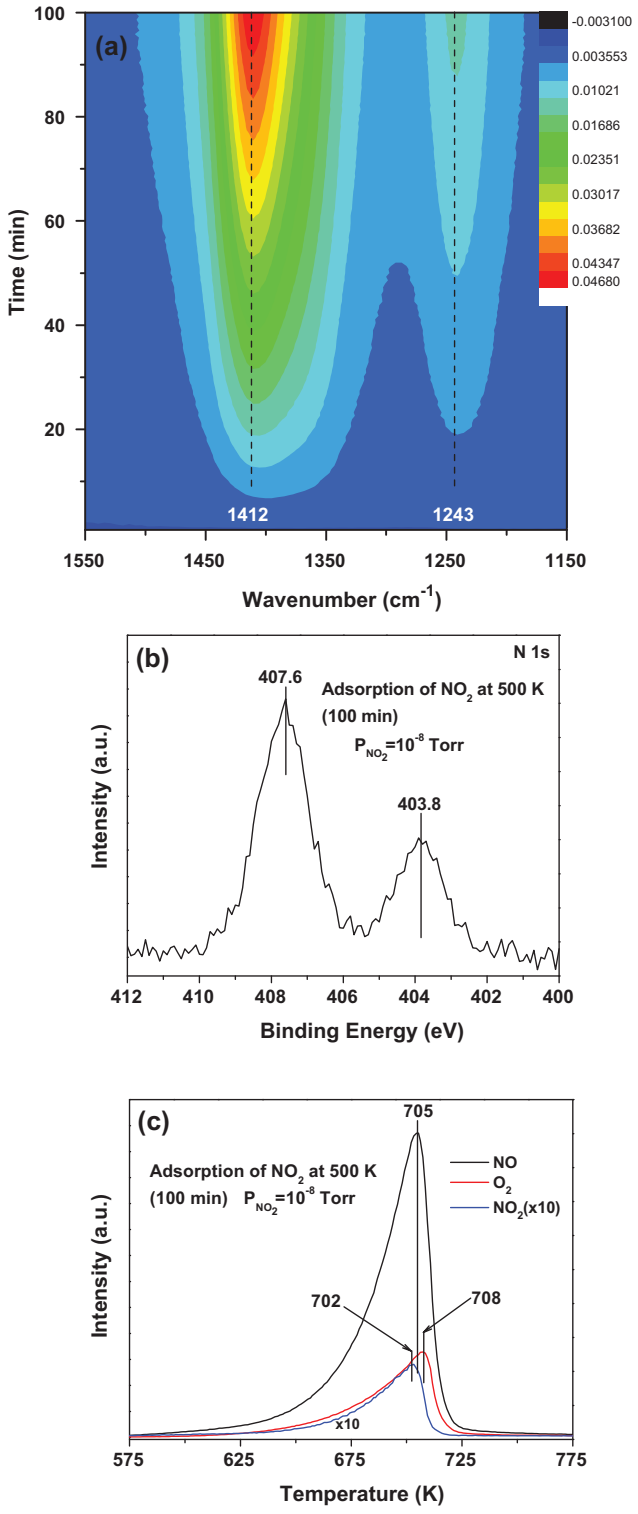

Fig. 1. (a) A contour plot of RAIR spectra recorded during the exposure of BaO/Pt(1 1 1) to NO_2 ($P_{NO_2} = 1.0 \times 10^{-8}$ Torr) as a function of time at 500 K (146 spectra were collected in 100 min). (b) N 1s XP spectrum for the system obtained following the exposure of BaO/Pt(1 1 1) to NO_2 ($P_{NO_2} = 1.0 \times 10^{-8}$ Torr; 100 min) at 500 K. (c) TPD spectra for the 30 (NO), 32 (O_2), and 46 (NO_2) amu mass fragments obtained from the system shown in panel b. (The NO_2 TPD spectrum is multiplied by a factor of 10).

403.8 eV as shown in Fig. 1b. Based on the previously reported XP binding energies, the N 1s peaks at 407.6 and 403.8 eV can be assigned to nitrates and nitrites, respectively [1,4,5,12,19]. These XPS results unambiguously show that nitrates have formed in larger amount than nitrites and the nitrites were not converted completely to nitrates at the conclusion of this experiment under the conditions applied. The O 1s XP spectrum (not shown) also substantiates that the thick BaO layer was not converted entirely to nitrites and nitrates, as substantial intensity remained at ~528.0 eV binding energy characteristic of O^{2-} ions in BaO. The formation of nitrites in significant amounts even at the high temperature of this study (i.e., 500 K) suggests that with the formation of $Ba(NO_3)_2$ clusters/particles the surface morphology changes significantly. As the nitrate clusters/particles form, new BaO layers become exposed to the incoming NO_2 reactants and form nitrites and subsequently nitrates.

TPD spectra of the 30 (NO), 32 (O_2), and 46 (NO_2) amu mass fragments obtained from this $Ba(NO_x)_2$ system shown in Fig. 1b are displayed in Fig. 1c. The maximum desorption rates for NO, O_2 and NO_2 were observed at 705, 708 and 702 K, respectively. In our earlier work we have established that nitrites were less thermally stable than nitrates, therefore, they decomposed at lower temperature during the TPD experiment than did nitrates [6]. The thermal decomposition processes of this nitrite/nitrate system can be described as follows.

The possible pathways for the thermal decomposition of nitrites are:

$$Ba(NO_2)_2 \rightarrow NO_2 + NO + BaO \quad (1)$$

$$2Ba(NO_2)_2 \rightarrow 4NO + O_2 + 2BaO \quad (2)$$

$$Ba(NO_2)_2 \rightarrow 2NO + BaO_2 \quad (2a)$$

$$2BaO_2 \rightarrow O_2 + 2BaO \quad (2b)$$

$$3Ba(NO_2)_2 \rightarrow 4NO + Ba(NO_3)_2 + 2BaO \quad (3)$$

The onset temperature of the NO desorption is 590 K (Fig. 1c), however, neither O_2 nor NO_2 evolution is detected below 625 K. This observation suggests that nitrites decompose by releasing only NO via reactions (2a) and/or (3). The formation of nitrates by the decomposition of nitrites through reaction (3) can be ruled out by the fact that no increase in the N 1s XP spectra of nitrates (data not shown) was observed upon annealing of this $Ba(NO_x)_2$ system. Therefore, the decomposition of nitrites most probably occurs according to reaction (2a). The BaO_2 formed in reaction (2a) releases O_2 according the reaction (2b), and these released O_2 contribute to the O_2 desorption feature at 708 K. The decomposition pathway of nitrites described above is in concert with that reported earlier for the NO_2-exposed BaO(~30 MLE)/Al_2O_3/NiAl(1 1 0) system [5].

The possible pathways for the thermal decomposition of nitrates are:

$$Ba(NO_3)_2 \rightarrow 2NO_2 + BaO_2 \quad (4)$$

$$2Ba(NO_3)_2 \rightarrow 4NO_2 + O_2 + 2BaO \quad (5)$$

$$2Ba(NO_3)_2 \rightarrow 4NO + 3O_2 + 2BaO \quad (6)$$

$$Ba(NO_3)_2 \rightarrow 2NO + O_2 + BaO_2 \quad (7)$$

$$Ba(NO_3)_2 \rightarrow NO_2 + NO + O_2 + BaO \quad (8)$$

Fig. 1c shows an NO_2 desorption feature with maximum desorption rate at 702 K, therefore, the decomposition of nitrates can occur via NO_2 release in accord with reaction (4). The thus formed BaO_2 can release O_2 by the reaction (2b) and leaves BaO behind. These two-step processes may be summarized in reaction (5). This nitrate decomposition mechanism is consistent with the experimental observation of simultaneous O_2 and NO_2 evolution during the decomposition of nitrates. Note that the NO_2 released from the decomposition of nitrates can dissociate in the mass spectrometer to produce NO and oxygen, which contributes to the NO desorption feature at 705 K. Since the trailing edge of the O_2 desorption feature closely follows that of the NO desorption trace, the decomposition of nitrates at higher temperature most probably occurs by the simultaneous release of $NO + O_2$ in accordance with reaction (6). The same path (reaction (6)) can also be achieved through reaction (7) if the BaO_2 formed in this reaction decomposes immediately to release O_2 according to reaction (2b). We can rule out the involvement of path (8) in the decomposition process because NO, O_2 and NO_2 desorption curves do not follow the same desorption path. Therefore, based on the observed TPD spectra, the nitrates in this $Ba(NO_x)_2$ system primarily decompose in two pathways releasing NO_2 (at lower temperature) and $NO + O_2$ (at higher temperature). This proposed decomposition scheme for the $Ba(NO_x)_2$ system is very similar to that put forward in our previous studies on $Ba(NO_x)_2$ systems [5,6,9]. First, nitrites decompose by releasing NO, which contributes to the low temperature tail of the NO desorption feature with maximum desorption rate at 705 K. Then nitrates dissociate via two pathways releasing NO_2 and $NO + O_2$. (In order to describe the decomposition patterns in a more quantitative manner deconvolution of the TPD traces would be necessary. However, due to the complexity of the decomposition process this could not be done with sufficient confidence).

The decomposition of nitrates via two pathways suggests the presence of two different types of nitrate species. However, in these experiments we could not differentiate and identify the two different nitrate species that decomposed to NO_2 only and $NO + O_2$. Previous studies on high surface area model catalysts have also shown both NO_2 and $NO + O_2$ as the primary products of low and high temperature decomposition of $Ba(NO_3)_2$, respectively [20,21]. Large aggregates (i.e., "bulk-like nitrates") were concluded to decompose to $NO + O_2$ at higher temperatures, while small aggregates or dispersed particles were proposed to decompose to NO_2 at lower temperatures. Decomposition of the dispersed phase at temperatures lower than that of bulk $Ba(NO_3)_2$ has been attributed to the strong interaction between the highly dispersed nitrate phase and the underlying substrate. However, in our model system with a thick BaO layer there is no strong interaction with the underlying Pt substrate. Therefore, the occurrence of decomposition of nitrates via two pathways in our model system may not be attributed to the presence of strong interactions with the underlying substrate that was reported for high surface area model catalysts.

3.2. Formation of $Ba(NO_x)_2$ at $P_{NO_2} = 1.0 \times 10^{-5}$ Torr and T = 500 K

In order to investigate the effect of NO_2 pressure on the formation of $Ba(NO_x)_2$ on BaO/Pt(1 1 1) NO_2 uptake was carried out at 1.0×10^{-5} Torr pressure and 500 K sample temperature. A series of IR spectra collected as a function of time (146 spectra in 100 min) during NO_2 adsorption ($P_{NO_2} = 1.0 \times 10^{-5}$ Torr) at 500 K are displayed in Fig. 2a as a contour plot in the frequency range of 1150–1550 cm^{-1}. The IR feature at 1245 cm^{-1} can be assigned to nitrites, whereas peaks at 1390, 1425 and 1460 cm^{-1} can be attributed to nitrates, as reported previously [1–3,5,6,15,17,18]. First, the IR peak intensities of both nitrite and nitrate species gradually increase with increasing NO_2 exposure time, and then the intensity of the nitrite feature starts decreasing. After about 5 min of NO_2 exposure, the nitrite feature at 1245 cm^{-1} completely disappears due to oxidation of nitrites to nitrates, whereas the intensities of nitrate IR features further increase with increasing NO_2 exposure. The IR features observed at 1390 and 1425 cm^{-1} after 100 min of NO_2 exposure have been assigned to crystalline nitrates [11,17,22,23]. The peak at 1460 cm^{-1}, which appears as a

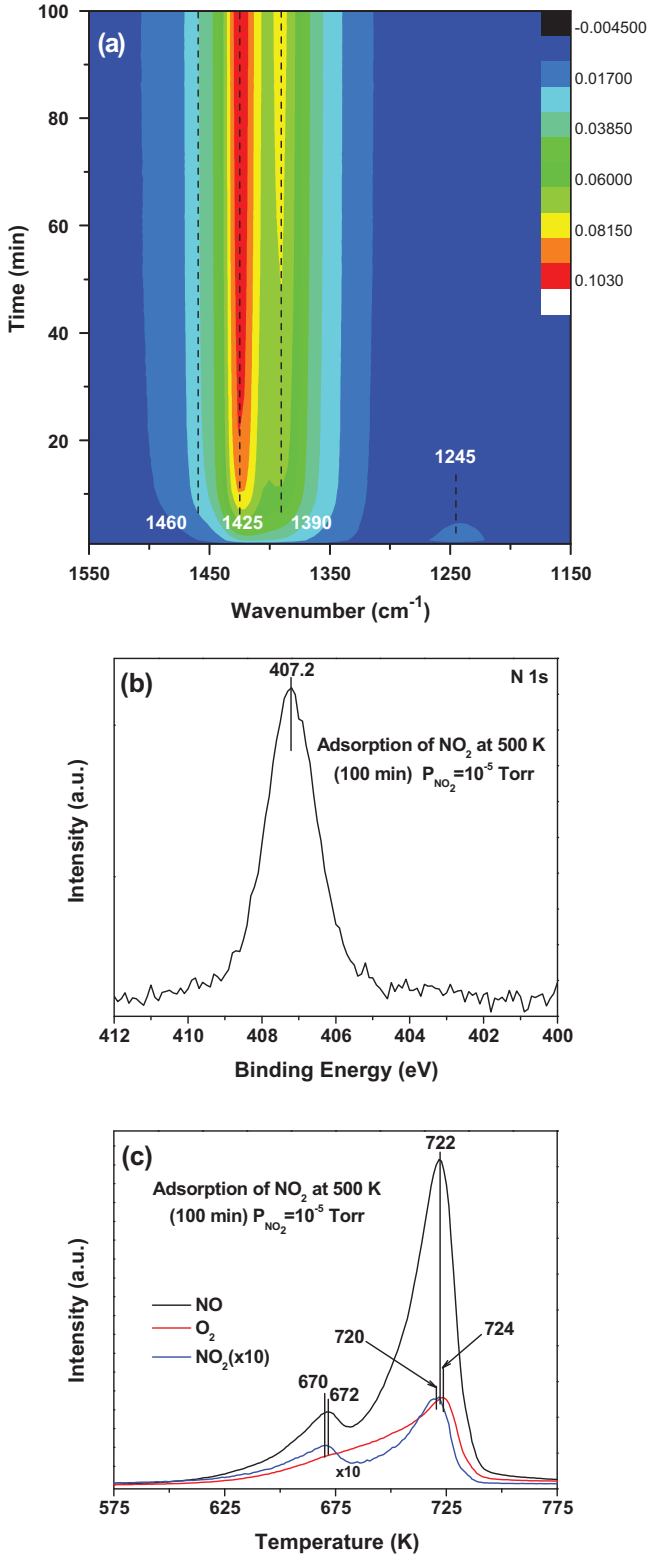

Fig. 2. (a) A contour plot of RAIR spectra recorded during the exposure of BaO/Pt(1 1 1) to NO_2 ($P_{NO_2} = 1.0 \times 10^{-5}$ Torr) as a function of time at 500 K (146 spectra were collected in 100 min). (b) N 1s XP spectrum for the system obtained following the exposure of BaO/Pt(1 1 1) to NO_2 ($P_{NO_2} = 1.0 \times 10^{-5}$ Torr; 100 min) at 500 K. (c) TPD spectra for the 30 (NO), 32 (O_2), and 46 (NO_2) amu mass fragments obtained from the system shown in panel b. (The NO_2 TPD spectrum is multiplied by a factor of 10).

shoulder in the IR spectrum (as shown in Figs. 3a and 5), is due to the overtone band of the in-plane bending mode ν_4 [18] of nitrate ions. The N 1s XP spectrum obtained following the exposure of BaO/Pt(1 1 1) to 1.0×10^{-5} Torr NO_2 for 100 min at 500 K shows one symmetric peak at 407.2 eV representing nitrate species [1,4,5,12,19]. These IRAS and XPS results unambiguously show that the initially formed nitrites can completely be oxidized to nitrates under the conditions applied, and only nitrates are present on the system at the saturation. The results in Figs. 1 and 2 also indicate that NO_2 pressures higher than 1.0×10^{-8} Torr is required for the complete oxidation of nitrites. The complete conversion of the thick BaO layer to $Ba(NO_3)_2$ was revealed by the complete absence of any trace of O^{2-} ions of BaO in the O 1s XP spectrum (O 1s spectra shown in Fig. 3) obtained at the conclusion of this experiment. (We have also investigated the formation of $Ba(NO_x)_2$ at 500 K following the exposure of BaO/Pt(1 1 1) to NO_2 in a wide pressure range of 1.0×10^{-8} to 1.0 Torr and the results obtained from these experiments (not shown) indicated that the complete oxidation of nitrites to nitrates and the full nitration of the thick (>20 MLE) BaO layer could only be achieved at $P_{NO_2} \geq 1.0 \times 10^{-5}$).

TPD spectra for the 30 (NO), 32 (O_2), and 46 (NO_2) amu mass fragments obtained from the $Ba(NO_3)_2$/Pt(1 1 1) system (corresponding N 1s XPS data is shown in Fig. 2b) are displayed in Fig. 2c. The NO TPD curve shows two distinct desorption features at 672 and 722 K, whereas the desorption of O_2 occurs at a maximum desorption rate of 724 K with a shoulder near 670 K. Similarly to NO, two NO_2 desorption features are observed at 670 and 720 K. These TPD spectra from this fully nitrated sample show that the nitrate decomposition occurs in two steps at temperature of ~670 K and ~720 K. The comparison of TPD traces displayed in Figs. 1c and 2c suggests that the mechanism of the decomposition process in each step of the system in Fig. 2c is similar to that described for the system in Fig. 1c. In each decomposition step nitrates decompose via two pathways by releasing NO_2 and $NO + O_2$. However, the decomposition temperature (~705 K) in Fig. 1c is between that of the low (~670 K) and high (~720 K) temperature desorption features of Fig. 2c. In order to obtain further insight into these two-step decomposition processes, we performed experiments with $Ba(NO_x)_2$ systems having different $Ba(NO_x)_2$ coverages and the results of these experiments are described in the following section.

3.3. *Thermal decomposition of $Ba(NO_x)_2$*

Five $Ba(NO_x)_2$ systems with different compositions (nitrite/nitrate ratios) were prepared via the adsorption of NO_2 on BaO/Pt(1 1 1) at 500 K to investigate the decomposition processes of nitrates. First we performed RAIRS and XPS experiments before the TPD scans for the characterization of the composition of each system. Fig. 3 shows a series of RAIRS (a), N 1s (b) and O 1s (c) XP spectra obtained from these $Ba(NO_x)_2$ systems (NO_2 exposure increases from system I to V). The IR spectrum for system I (orange spectrum) in Fig. 3a shows peaks at 1414 and 1243 cm^{-1} for nitrates and nitrites, respectively. Our previous studies showed the formation of amorphous nitrates following the exposure of a thick BaO layer to elevated NO_2 pressure (up to 1.0 Torr) at 300 K and its conversion to crystalline phase upon annealing to 500 K in the absence of gas phase NO_2 [11,17]. In the present experiments, the thick BaO layer was exposed to an elevated NO_2 pressure at 500 K, therefore, crystalline nitrates could form directly. However, the IR spectrum for nitrates in system I shows a single, although asymmetric peak (with a shoulder at its low frequency side) at 1414 cm^{-1}, which is different from the characteristic IR spectrum for crystalline, as well as amorphous nitrates formed on thick BaO as shown by our previous studies [11,17]. (This IR feature, on the other hand, is very similar to that we have obtained in a cyclic, room temperature NO_2 adsorption/575 K anneal, experiment over a thick (>30 MLE) BaO

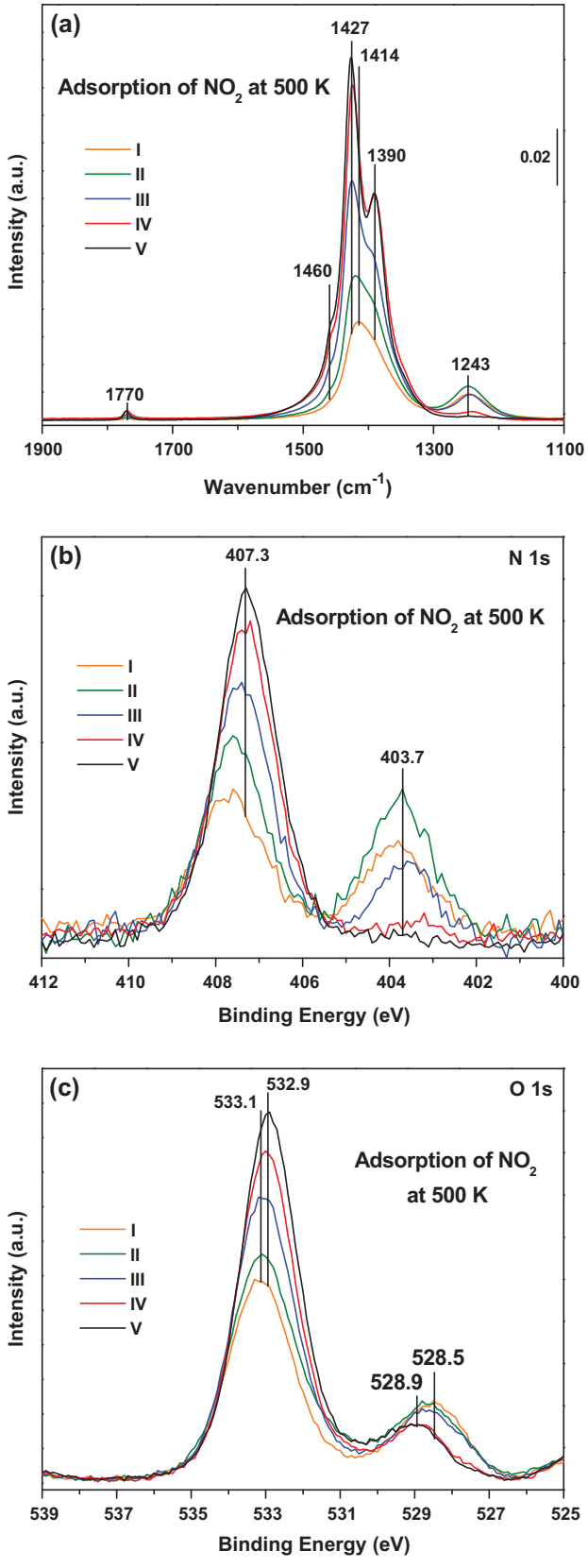

Fig. 3. A series of RAIRS (a), N 1s (b) and O 1s (c) XP spectra obtained for five $Ba(NO_x)_2$/Pt(1 1 1) systems(I–V), which are prepared by NO_2 exposure at 500 K. The $Ba(NO_x)_2$ coverage increases from system I (orange) to V (black). (NO_2 exposures: I—1.0×10^{-5} Torr for 1 min; II—1.0×10^{-6} Torr for 20 min; III—1.0×10^{-6} Torr for 40 min; IV—2.0×10^{-5} Torr for 30 min; V—5.0×10^{-5} to 1.0×10^{-4} Torr for 20 min).

layer supported on a 12 ML Al_2O_3 film on NiAl(1 1 0) [6]. This IR feature in that study was assigned to nitrates in small $Ba(NO_3)_2$ clusters/particles.) The IR spectrum for crystalline nitrates show two resolved IR features at ~1427 and ~1390 cm^{-1} as shown in Figs. 2, 3a and 5 as well as in previous studies [11,17,22–24]. The amorphous nitrate layer formed on thick BaO at 300 K has been shown to exhibit peaks at ~1335 and ~1465 cm^{-1} [11,17]. Although the two IR features at ~1427 and ~1390 cm^{-1} are not resolved for system I, the other two IR features characteristic of crystalline nitrates at 1770 cm^{-1} and 2400 cm^{-1} (not shown) are present. The absence of IR features characteristic of amorphous nitrates (broad IR bands at ~1465 and ~1335 cm^{-1}) in system I further suggests that the nitrates in system I are crystalline in nature. The appearance of the broad single peak at 1414 cm^{-1} (instead of two resolved features at ~1427 and ~1390 cm^{-1} for crystalline nitrates) in system I is most likely due to the disorder in the crystalline phase at 500 K. Previous studies on bulk nitrates also showed the appearance of a disorder in the crystal structure at about 573 K temperature, which leads to the variations in the spectral parameters for the $(\nu_1 + \nu_4)$, $2\nu_1$, $(\nu_1 + \nu_3)$ and $2\nu_3$ vibrations [25]. In addition, dielectric constant and dc resistivity measurements of the barium nitrate showed the existence of thermal hysteresis accompanying the phase transformation, which occurs at 416 K [26]. The presence of orientational disorder of the nitrate group leading to order–disorder phase transition of $Ba(NO_3)_2$ was reported based on the observed sharp peak about 573 K in the thermomechanical analysis curve [27]. However, these studies did not report the changes in the fundamental vibrations in the frequency range of 1300–1500 cm^{-1}. Therefore, the origin and nature of the disorder in the crystal structure of crystalline nitrates in system I may be different from that reported for bulk crystalline nitrates. These deviations are most likely to due to the fundamental differences between the two systems with respect to the structures of nitrates in bulk powder sample and thin nitrate film/nitrate nanoparticles. The formation of very small $Ba(NO_3)_2$ clusters/particles would explain the broad IR features obtained from this sample. These small particles may be stabilized by the underlying, unreacted BaO layer, as we have seen it in our previous study [17]. When a thick (~30 MLE) BaO film was exposed to NO_2 at elevated pressures (~1×10^{-4} Torr), large amount of amorphous $Ba(NO_3)_2$ formed as evidenced by the intense IR bands at 1466 and 1335 cm^{-1}. The IR feature at ~1770 cm^{-1} of the crystalline $Ba(NO_3)_2$ was completely absent. Furthermore, the O 1s XP spectrum had still significant contribution from unreacted BaO. When this system was gradually annealed to 600 K the IR spectra changed dramatically, i.e., the intensities of the two bands of the amorphous nitrate phase decreased, and a broad asymmetric band, centered at 1429 cm^{-1} with a shoulder at 1390 cm^{-1}developed, and increased in intensity with increasing annealing temperature up to 600 K. But the sharp and resolved two IR features of large crystalline $Ba(NO_3)_2$ particles were not seen. However, when the thick BaO layer was completely converted to amorphous $Ba(NO_3)_2$ (under 1 Torr of NO_2 at 300 K), the onset temperature of the ordered crystalline phase formation (i.e., the appearance of the sharp IR bands at 1430 and 1392 cm^{-1}) was around 450 K, and it was fast at 500 K (although it took more than 20 min for complete crystallization to occur) [11]. Based on the results of these studies, we assign the IR feature at 1414 cm^{-1} to small, disordered crystalline nitrate particles in system I. Most likely the formation of these small, disordered crystalline nitrate clusters occurs at the onset of NO_2 exposure at 500 K. With increasing NO_2 exposure, more nitrate clusters form and begin to agglomerate to form large, ordered crystalline nitrate particles. This process ultimately leads to the splitting of the IR feature at 1414 cm^{-1} to two features at 1427 and 1390 cm^{-1}, as seen for systems IV and V. The agglomeration of small nitrate clusters to form large particles with increasing NO_2 exposure ($Ba(NO_3)_2$

coverage) has also been reported previously in studies on BaO-based model systems [6,10,17]. In addition to the development of the sharp features of crystalline $Ba(NO_3)_2$, the nitrite feature at 1243 cm^{-1} completely disappeared due to the full conversion of nitrites to nitrates at the highest NO_2 exposure (black spectrum; system V). It should be noted that in order to achieve a high $Ba(NO_3)_2$ coverage that initiates the agglomeration of small, disordered crystalline clusters into large, well-ordered crystalline aggregates, NO_2 pressures higher than 1.0×10^{-7} Torr have to be applied at 500 K sample temperature. At $P_{NO_2} = 1.0 \times 10^{-8}$ Torr, this splitting of the IR peak is not observed as shown in Fig. 2, but at 1.0×10^{-7} Torr this splitting is seen (not shown). The shoulder at 1460 cm^{-1} in the IR spectrum can be assigned to the overtone band of the in plane bending mode ($2\nu_4$) as described in the previous section. The weak feature at 1770 cm^{-1} is assigned to the combination band of the symmetric NO stretching mode (ν_1) and the in-phase deformation (ν_4) [1] of crystalline $Ba(NO_3)_2$, as this peak has been observed at 1774, and 1780 cm^{-1} in the powder $Ba(NO_3)_2$ samples [28,29]. Furthermore, a weak feature is observed near 2400 cm^{-1} (not shown) for the combination band of the symmetric and asymmetric NO stretching modes ($\nu_1 + \nu_3$) [25]. In a study by Coronado and Anderson, the IR features at 1460, 1775 and 2400 cm^{-1} were also observed after annealing of $Ba(NO_3)_2$ formed on $BaCl_2/SiO_2$ at room temperature to 563 K [23]. In addition, they also observed the sharpening and shifting of the IR peaks observed at 1360 and 1460 cm^{-1} for amorphous nitrates upon annealing to 563 K. Note that the positions of the observed IR peaks at 1770, 1427 and 1390 cm^{-1} in our study are very similar to those reported for bulk crystalline nitrates [25,29,30] indicating the formation of bulk crystalline nitrates on this model BaO/Pt(1 1 1) system.

Fig. 3b shows the N 1s XP spectra corresponds to the systems in Fig. 3a. The N 1s XP spectrum for system I (orange spectrum) shows peaks at 407.3 and 403.7 for nitrates and nitrites, respectively. With increasing NO_2 exposure, both nitrite and nitrate intensities increase initially, and then the nitrite peak intensity begins to decrease, due to the nitrite-to-nitrate conversion. At the highest NO_2 exposure (black spectrum; system V), only nitrates are present in the system. The disappearance of the N 1s XPS trace of nitrites coincides with the development of the two sharp IR features of crystalline $Ba(NO_3)_2$. Fig. 3c shows the O 1s XP spectra corresponding to the $Ba(NO_x)_2$ systems in Fig. 3a and b. The O 1s XP spectrum for system I (orange spectrum) shows peaks at 533.1 and 528.5 eV. The peak at 533.1 eV can be assigned to oxygen in nitrates and nitrites, whereas the peak at 528.5 eV represents O^{2-} in BaO. With increasing NO_2 exposure, the intensity of the O 1s peak for $Ba(NO_x)_2$ increases and that for BaO decreases due to the conversion of BaO to $Ba(NO_x)_2$. In addition, an O 1s peak appears at 528.9 eV for O of Pt-oxide-like domains formed under elevated NO_2 pressures and temperature (500 K) [31]. At the highest NO_2 exposure (black spectrum; system V), the BaO layer was completely converted to $Ba(NO_3)_2$ and the O 1s peaks centered at 532.9 and 528.9 eV represent nitrates and Pt-oxide domains, respectively.

Fig. 4 shows the TPD spectra for the 30 (NO) (a), 32 (O_2) (b), and 46 (NO_2) (c) amu mass fragments obtained from the systems (I–V) shown in Fig. 3. At the lowest NO_2 exposure (orange spectra; system I), NO, O_2 and NO_2 desorption features are all seen with maximum desorption rates at ~700 K. With increasing NO_2 exposure, the maximum desorption rates shift to higher temperatures as the nitrite/nitrate coverage increases, while a lower temperature desorption feature develops in each TPD trace. TPD curves for both NO and NO_2 (but not O_2) show low temperature desorption features at ~615 K for system II (green curve), although with very low intensities. For system III (blue spectra) NO, NO_2 as well as O_2 desorption features are observed at 656, 654 K and 658 K, respectively. With increasing NO_2 exposure, the lower temperature desorption features shift dramatically to higher temperatures (from 615 K for system I to ~690 K for system V). At the highest NO_2 exposure the maximum desorption rates of NO, O_2 and NO_2 are observed at 729, 731 and 727 K, respectively, for the high temperature desorption process. For the low temperature desorption the NO, O_2 and NO_2 peak maxima are observed at 692, 701 and 690 K, respectively. These two-step decomposition processes occur by releasing NO_2 and $NO + O_2$ in each step at two different temperature regions as described in the previous sections.

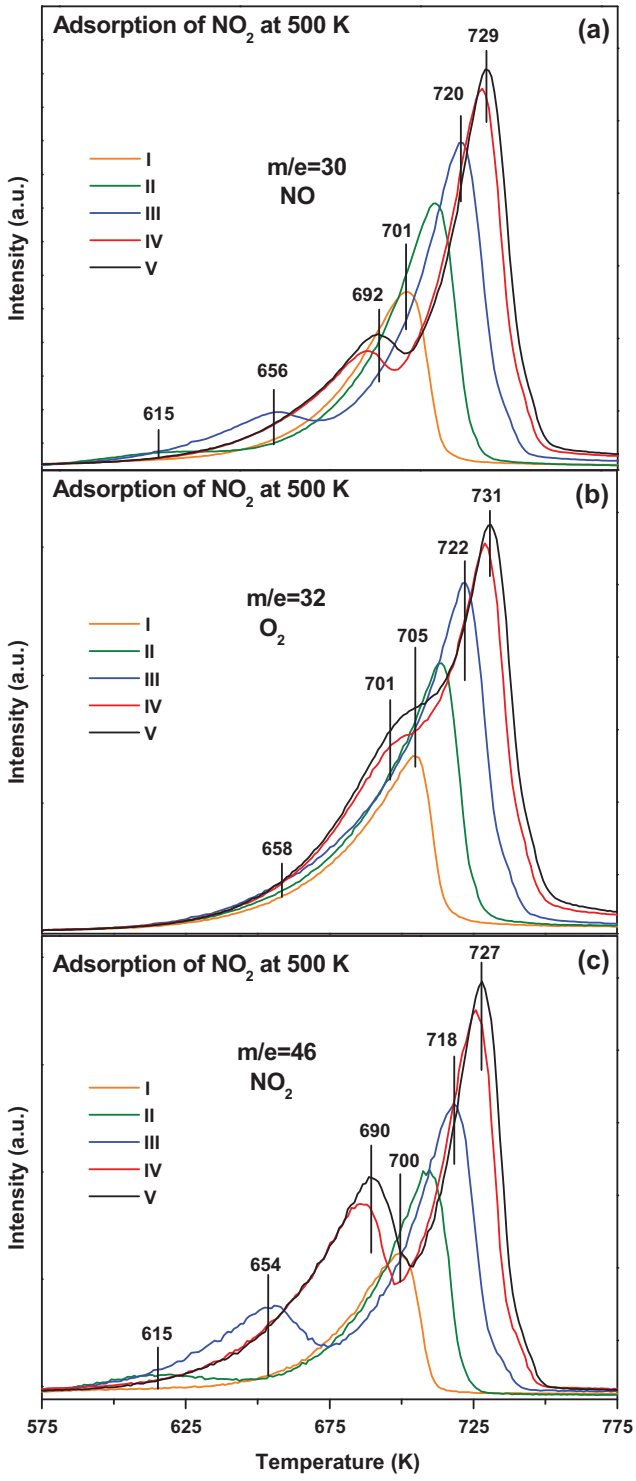

Fig. 4. TPD spectra for the 30 (NO) (a), 32 (O_2) (b), and 46 (NO_2) (c) amu mass fragments obtained from the $Ba(NO_x)_2$/Pt(1 1 1) systems (I–V)shown in Fig. 3. (The NO_2 TPD spectra are multiplied by a factor of 10).

The two-step decomposition process in two temperature regions can be explained by the proposed two-phase (ordered and disordered) crystalline nitrate system. At low NO_2 exposures, small disordered crystalline nitrate particles form on the surface and their decomposition occurs via two pathways with the release of NO_2, and $NO + O_2$ during the temperature ramp. Nitrites (present in systems I–III) decompose with the release of NO only. With increasing NO_2 exposure, the unreacted BaO and surface nitrites convert to small, disordered crystalline nitrate clusters, which, ultimately, agglomerate to form large, well-ordered crystalline nitrates. The appearance of the low temperature decomposition feature in the TPD spectra, therefore, can be associated with the formation of large crystalline $Ba(NO_3)_2$ particles. The two processes that take place during the NO_2 exposure of the sample at 500 K are the formation of nitrites/nitrates, and the agglomeration of small $Ba(NO_3)_2$ clusters into large crystallites. At 500 K sample temperature in these experiments the formation of small $Ba(NO_3)_2$ clusters/particles is faster than the agglomeration of these particles into large crystals. At this temperature, the conversion of a significant fraction of the BaO film into $Ba(NO_3)_2$ is required for the formation of large crystallites. The comparison of IR and TPD spectra in Figs. 3a and 4, respectively, indicates that the development of the low-temperature desorption feature can be correlated with the splitting of the nitrate IR feature at ~1415 cm^{-1}. For system I (orange spectra), the IR spectrum in Fig. 3a shows a single nitrate peak at 1414 cm^{-1}, while the low-temperature desorption features of NO, O_2 and NO_2 are absent in the TPD spectra in Fig. 4. The IR spectrum for system II (green spectrum) shows the initiation of the splitting of the IR feature at 1414 cm^{-1} to two features at 1427 and 1390 cm^{-1}, and, concomitantly, the development of low-temperature desorption features is observed in the TPD spectra of Fig. 4. At even higher NO_2 exposures, as the concentration of small nitrate particles increases, the formation of large, well-ordered crystalline nitrate particles accelerates. These larger, well-structured crystalline-nitrate particles generate an IR spectrum with two distinct features at 1390 and 1427 cm^{-1} as shown by the Fig. 3a (black spectrum; system V). During the TPD experiment these large crystalline-nitrate particles formed at 500 K start to decompose (low-temperature decomposition feature) and convert back to small, disordered-crystalline clusters. The TPD results suggest, that the two nitrate phases (disordered and ordered crystalline $Ba(NO_3)_2$) possess different thermal stabilities. The ordered phase seems to be the less stable one, and starts to decompose at lower temperature. However, before it could decompose completely, it transforms into the disordered phase. The decomposition temperature of this disordered phase is higher, resulting in the high temperature decomposition peaks in the TPD spectra. In order to further confirm the order to disorder crystalline-nitrate phase transition, we collected IR spectra after annealing the fully nitrated, well-ordered system (formed at 500 K) to different temperatures, and the results obtained are shown in Fig. 5. (The system shown in Fig. 5 was prepared under identical conditions to system V in Figs. 3 and 4.) The well-ordered crystalline nitrate particles formed at 500 K show two resolved features at 1427 and 1390 cm^{-1} in the IR spectrum. This IR spectrum does not change upon annealing to 600 K, since no decomposition of nitrates occurs in agreement with the TPD spectra shown in Fig. 4 (black spectra; system V). However, annealing to 700 K leads to the partial decomposition of the large, well-ordered crystalline particles and mostly to the formation of small, disordered crystalline clusters. The IR spectrum obtained after annealing to 700 K shows a single IR peak at 1415 cm^{-1}, consistent with collapse of the ordered nitrate phase and the formation of the disordered phase, the reverse process we have discussed above for the NO_2 uptake. The IR spectrum recorded at 500 K after flashing the sample to 700 K is practically identical to that obtained for system I, i.e., before the formation of large, well-ordered crystalline particles (see Fig. 3a). No IR features were

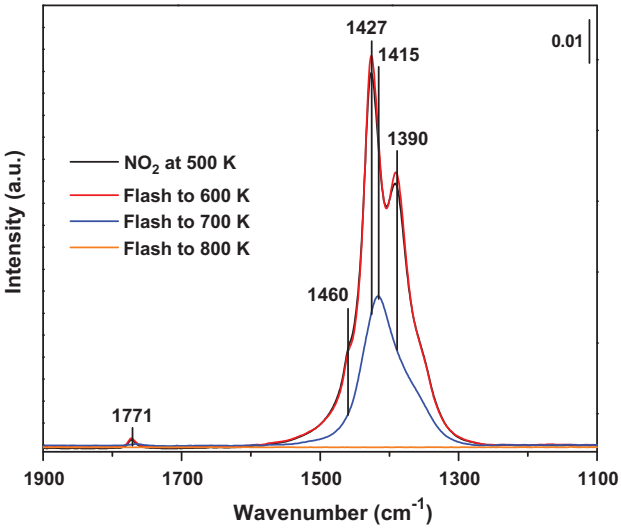

Fig. 5. A series of IR spectra obtained following annealing of the nitrate system with well-ordered, bulk crystalline nitrate particles formed at 500 K to the specified temperatures. The $Ba(NO_3)_2$ system obtained following the exposure of BaO/Pt(1 1 1) to NO_2 at 500 K is similar to the system V in Figs. 3 and 4. All the spectra were collected at 500 K.

detected after annealing to 800 K due to the complete decomposition of nitrates, in concert with the TPD spectra shown in Fig. 4. This proposed mechanism explains the experimentally observed two-step decomposition process of the nitrates formed after the thick BaO film was exposed to NO_2 at elevated pressures and at 500 K. The decomposition pathway (the observation of both NO and NO_2 evolution during crystalline $Ba(NO_3)_2$ decomposition in both steps) we have observed in this study, however, is different from that commonly accepted for the decomposition of bulk $Ba(NO_3)_2$ (only $NO + O_2$ evolution). Experiments aimed at understanding the possible effects of the metal support (here Pt), and the peroxides and oxide layers (BaO_2 and BaO formed during the decomposition process) on the thermal decomposition of crystalline $Ba(NO_3)_2$ are currently under way.

4. Conclusions

The exposure of BaO (>20 MLE)/Pt(1 1 1) to 1.0×10^{-8} Torr NO_2 pressure at 500 K leads to the formation of a $Ba(NO_x)_2$ layer with small disordered-crystalline nitrate clusters. Under these conditions only the top portion of BaO converts to $Ba(NO_x)_2$ due to the diffusion limitation of NO_2 through the top $Ba(NO_x)_2$ layers. The nitrites in this $Ba(NO_x)_2$ layer stay without converting completely to nitrates even after 100 min of NO_2 exposure ($(P_{NO_2} = 1.0 \times 10^{-8}$ Torr and $T = 500$ K). In the thermal decomposition of $Ba(NO_x)_2$, first nitrites decompose desorbing NO and the decomposition of nitrates occurs releasing NO_2 and $NO + O_2$. At 500 K and $P_{NO_2} \geq 1.0 \times 10^{-7}$ Torr, first NO_2 reacts with BaO to form small disordered-crystalline $Ba(NO_3)_2$ particles and the IR spectrum of this system shows only one feature at ~1414 cm^{-1} due to the disordered crystal structure. With increasing NO_2 exposure, more small disordered crystalline $Ba(NO_3)_2$ particles are generated, which initiates the agglomeration of small clusters into large, well-ordered bulk crystalline nitrate particles, characterized by IR peaks at ~1390 and 1427 cm^{-1}. The positions of the IR peaks observed for these well-ordered bulk-crystalline nitrate aggregates on our model system are very similar to those reported for bulk crystalline samples indicating the formation of bulk crystalline-nitrates under the conditions applied. The thermal decomposition of these well-structured, bulk crystalline nitrate particles occurs in

two steps, releasing NO_2 and $NO + O_2$ in each step. NO_2 pressures $\geq 1.0 \times 10^{-5}$ Torr is required for the complete oxidation of initially formed nitrites to nitrates and the full nitration of the BaO layer at 500 K.

Acknowledgments

We gratefully acknowledge the US Department of Energy (DOE), Office of Basic Energy Sciences, Division of Chemical Sciences for the support of this work. The research described in this paper was performed at the Environmental Molecular Sciences Laboratory (EMSL), a national scientific user facility sponsored by the DOE Office of Biological and Environmental Research and located at Pacific Northwest National Laboratory (PNNL). PNNL is operated for the US DOE by Battelle Memorial Institute under contract number DE-AC05-76RL01830.

References

[1] A. Desikusumastuti, M. Happel, K. Dumbuya, T. Staudt, M. Laurin, J.M. Gottfried, H.-P. Steinruck, J. Libuda, J. Phys. Chem. C 112 (2008) 6477–6486.
[2] A. Desikusumastuti, M. Laurin, M. Happel, Z. Qin, S. Shaikhutdinov, J. Libuda, Catal. Lett. 121 (2008) 311–318.
[3] A. Desikusumastuti, T. Staudt, H. Grönbeck, J. Libuda, J. Catal. 255 (2008) 127–133.
[4] T. Staudt, A. Desikusumastuti, M. Happel, E. Vesselli, A. Baraldi, S. Gardonio, S. Lizzit, F. Rohr, J. Libuda, J. Phys. Chem. C 112 (2008) 9835–9846.
[5] C.-W. Yi, J.H. Kwak, J. Szanyi, J. Phys. Chem. C 111 (2007) 15299–15305.
[6] C.-W. Yi, J. Szanyi, J. Phys. Chem. C 113 (2009) 2134–2140.
[7] M. Bowker, P. Stone, R. Smith, E. Fourre, M. Ishii, N.H. de Leeuw, Surf. Sci. 600 (2006) 1973–1981.
[8] M. Bowker, M. Cristofolini, M. Hall, E. Fourre, F. Grillo, E. McCormack, P. Stone, M. Ishii, Top. Catal. 42–43 (2007) 341–343.
[9] K. Mudiyanselage, C.W. Yi, J. Szanyi, Langmuir 25 (2009) 10820–10828.
[10] P. Stone, M. Ishii, M. Bowker, Surf. Sci. 537 (2003) 179–190.
[11] K. Mudiyanselage, C.-W. Yi, J. Szanyi, Phys. Chem. Chem. Phys. 13 (2011) 11016.
[12] A. Tsami, F. Grillo, M. Bowker, R.M. Nix, Surf. Sci. 600 (2006) 3403–3418.
[13] C.W. Yi, J.H. Kwak, C.H.F. Peden, C.M. Wang, J. Szanyi, J. Phys. Chem. C 111 (2007) 14942–14944.
[14] A. Desikusumastuti, Z. Qin, M. Happel, T. Staudt, Y. Lykhach, M. Laurin, F. Rohr, S. Shaikhutdinov, J. Libuda, Phys. Chem. Chem. Phys. 11 (2009) 2514–2524.
[15] A. Desikusumastuti, T. Staudt, M. Happel, M. Laurin, J. Libuda, J. Catal. 260 (2008) 315–328.
[16] E. Ozensoy, C.H.F. Peden, J. Szanyi, J. Catal. 243 (2006) 149–157.
[17] C.-W. Yi, J. Szanyi, J. Phys. Chem. C 113 (2009) 716–723.
[18] H. Hesske, A. Urakawa, A. Baiker, J. Phys. Chem. C 113 (2009) 12286–12292.
[19] P. Schmitz, R. Baird, J. Phys. Chem. B 106 (2002) 4172–4180.
[20] X. Chen, J. Schwank, J. Li, W.F. Schneider, C.T. Goralski Jr., P.J. Schmitz, Appl. Catal. B: Environ. 61 (2005) 164–175.
[21] X. Chen, J. Schwank, J. Li, W.F. Schneider, J.C.T. Goralski, P.J. Schmitz, J. Mater. Chem. 15 (2005) 366–368.
[22] P. Broqvist, H. Gronbeck, E. Fridell, I. Panas, J. Phys. Chem. B 108 (2004) 3523–3530.
[23] J.M. Coronado, J.A. Anderson, J. Mol. Catal. A: Chem. 138 (1999) 83–96.
[24] K. Mudiyanselage, C.-W. Yi, J. Szanyi, J. Phys. Chem. C 114 (2010) 16955–16963.
[25] S. Taha, M. Tosson, Thermochim. Acta 236 (1994) 217–226.
[26] F. El-Kabbany, G. Said, S. Mahrous, N.H. Taher, Phys. Status Solidi (A) 99 (1987) 105–113.
[27] Y.A. Badr, R. Kamel, J. Phys. Chem. Solids 41 (1980) 1127–1131.
[28] M.H. Brooker, D.E. Irish, G.E. Boyd, J. Chem. Phys. 53 (1970) 1083–1087.
[29] E. Roedel, A. Urakawa, S. Kureti, A. Baiker, Phys. Chem. Chem. Phys. 10 (2008) 6190–6198.
[30] A.M. Bon, C. Benoit, O. Bernard, Phys. Status Solidi B-Basic Res. 78 (1976) 67–78.
[31] K. Mudiyanselage, J.F. Weaver, J. Szanyi, J. Phys. Chem. C 115 (2011) 5903.